Am J Transl Res 2017;9(7):3245-3257
www.ajtr.org /ISSN:1943-8141/AJTR0054241

Original Article

Light of DNA-alkylating agents in castration-resistant prostate cancer cells: a novel mixed EGFR/DNA targeting combi-molecule

Guan-Can Liang[1*], Hao-Feng Zheng[1*], Yan-Xiong Chen[1], Teng-Cheng Li[1], Wei Liu[2], You-Qiang Fang[1]

[1]*Department of Urology, The Third Affiliated Hospital of Sun Yat-sen University, Guangzhou 510630, China;* [2]*Guangdong Provincial Key Laboratory of Liver Disease, The Third Affiliated Hospital of Sun Yat-sen University, Guangzhou 510630, China.* [*]*Equal contributors.*

Received March 22, 2017; Accepted July 5, 2017; Epub July 15, 2017; Published July 30, 2017

Abstract: Objective: The mechanism underlying the therapeutic effects of combi-molecule JDF12 on prostate cancer (PCa) DU145 cells remains still unclear. This study aimed to investigate the proteomic profile after JDF12 treatment in DU145 cells by comparing with that in Iressa treated cells and untreated cells. Methods: MTT was used to evaluate drug cytotoxicity, DAPI staining was done to assess apoptosis of cells, and flow cytometry was used to analyze cell cycle. iTRAQ and qPCR were employed to obtain the proteomic profiles of JDF12 treated, Iressa treated, and untreated DU145 cells, and validate the expression of selected differentially expressed proteins, respectively. Results: JDF12 could significantly inhibit the proliferation and increase the apoptosis of DU145 cells when compared with Iressa or blank group. In total, 5071 proteins were obtained, out of which, 42, including 21 up-regulated and 21 down-regulated proteins, were differentially expressed in JDF12 group when compared with Iressa and blank groups. The up-regulated proteins were mainly involved in DNA damage/repair and energy metabolism; while the down-regulated proteins were mainly associated with cell apoptosis. qPCR confirmed the expression of several biologically important proteins in DU145 cells after JDF12 treatment. Conclusion: The molecular mechanisms of DNA alkylating agents on PCa therapy that with the assistant of EGFR-blocker were revealed on proteomic level, which may increase the possible applications of DNA alkylating agents and JDF12 on PCa therapy.

Keywords: DNA alkylating agents, JDF12, Iressa, iTRAO, prostate cancer

Introduction

Prostate cancer (PCa) is the most common solid organ malignancy in the United States and remains the second leading cause of cancer related death in American men [1]. Approximately, 180,000 new cases of PCa and over 26,000 deaths were estimated in the US in 2016 [2]. PCa related deaths are typically the result of metastatic castration-resistant prostate cancer (mCRPC), and historically the median survival time of patients with mCRPC is less than two years [3].

Treatment of mCRPC patients has dramatically changed over the past decade. Targeted therapy is the leading treatment of mCRPC, especially that targeting androgen receptor (AR) including abiraterone, cabazitaxel, and enzalutamide. However, most patients ultimately progress to an advanced stage of PCa and experience severe toxic side effects upon treatment [4].

DNA-alkylating drugs, which can kill cancer cells by functioning to primarily cause DNA damage in cells, have been widely used in the treatment of different cancers. However, they have several limitations: they may damage normal cells and cause severe toxicity and other side effects [5]. The unclear mechanisms also prevent DNA-alkylating drugs from further development.

In our previous studies [6, 7], a novel mixed epidermal growth factor receptor EGFR/DNA targeting combi-molecule (JDF12) was designed and results showed it could block EGFR-mediated signaling and also alkylate DNA. JDF12 was associated with less side effects as well

as low drug-resistant rate when compared with Iressa. However, the differences in proteomics and potential molecular mechanisms of biological effects between JDF12 and Iressa are still poorly understood.

This study was performed to investigate proteomic profiles of JDF12 and Iressa treated DU145 cells, aiming to reveal the potential molecular mechanisms underlying the therapeutic effects of JDF12.

Methods and materials

Drug treatment

JDF12 was synthesized by Prof Bertand Jeanlaude in the Cancer Drug Research Laboratory Department of Medicine, McGill University Health Centre. Iressa and mitozolomide (MTZ) were purchased from Sigma (USA). Drugs were dissolved in dimethyl sulfoxide (DMSO) to prepare a 50 mM stock solution which was then stored at -20°C. The solution was diluted in RPMI-1640 with 10% fetal bovine serum (FBS) before use. The final DMSO concentration was lower than 0.2%.

Cell culture

The Human PCa DU145 cells were obtained from the Cell Bank of the Chinese Academy of Sciences (Shanghai, China). Cells were cultured in RPMI-1640 (Gibico, USA) with 10% FBS (PAN, Germany), 100 U/mL penicillin and 100 μg/mL streptomycin at 37°C in a humidified atmosphere of 5% CO_2 in air.

Cell cytotoxicity assay

The viability of DU145 cells was assessed by MTT (Sigma, USA) assay. In brief, cells were plated at a density of 5×10^3/well in 96-well plate. After overnight incubation, cells were treated with different drugs at different concentrations (0.003 μM, 0.016 μM, 0.08 μM, 0.4 μM, 2 μM, 10 μM, and 50 μM). In blank group, cells were treated with RPMI-1640 with 10% FBS of equivalent volume. After incubation for 24 h, 48 h, and 72 h, MTT solution was added into each well (final concentration: 0.5 mg/mL), followed by incubation for another 4 h. Then, the medium was removed, and 150 μL of DMSO was added. After incubation for 15 min, the optical density (OD) was measured on a microplate reader (BioRab, USA) at 490 nm.

DAPI staining

The apoptosis morphology was evaluated by DAPI staining (KeyGEN BioTECH, Jiangsu, China). The IC_{50} concentration at 48 h was determined in pilot study. In brief, 2×10^5 cells were exposed to JDF12 at this IC_{50} for 0 h, 12 h, 24 h, and 48 h. Then, cells were washed with phosphate-buffered saline (PBS) once and stained with DAPI (300 nmol/L) for 10 min. After washing with methanol, cells were observed under a fluorescence microscope (Nikon, Japan).

Cell cycle analysis

The effects of JDF12 and Iressa on the cell cycle were evaluated by flow cytometry. Du145 cells were seed in 6-well plates at a density of 2×10^5 cells/well. After overnight incubation, cells were treated with JDF12 or Iressa for different duration (0 h, 12 h, 24 h, and 48 h). Cells were collected and fixed with 70% ice-cold ethanol at 4°C overnight. Then, cells were re-suspended and incubated with 100 μL of RNase (0.5 mg/mL) for 30 min at 37°C. After addition of 400 μl of propidium iodide (cell cycle detection kit, KeyGEN BioTECH, Jiangsu, China), incubation was performed at 4°C for 30 min in dark. The cell cycle was detected by flow cytometry (FACSCalibur, Becton Dickinson, SanJose, CA, USA), and data were analyzed with ModFit software.

Protein extraction, digestion and iTRAQ labeling

1×10^6 DU145 cells were seeded in 75-cm^2 flasks. After incubation for 24 h, cells were treated with JDF12 or Iressa at IC_{50} for 48 h. In blank group, the medium of equivalent volume was added. After 24-h incubation, cells were washed twice with ice-cold PBS and lysed with RIPA (KeyGEN BioTECH, Jiangsu, China). Then, lysates were centrifuged at 12000 × g for 20 min at 4°C. The protein concentration was measured by BCA kit (KeyGEN BioTECH, Jiangsu, China). Proteins were stored at -80°C for further use.

Proteins were subjected to tryptic hydrolysis with a modified filter-aided sample preparation (FASP) protocol. 200 μg of proteins in each group was incubated with 4 μL of Reducing Reagent (AB Sciex, Dublin, CA, USA) for 1 h at 60°C, followed by treatment with 2 μL of Cy-

Table 1. Primers used for quantitative qPCR

Gene	Forward	Reverse
HK2	GACCAACTTCCGTGTGCTTT	TCCATGAAGTTAGCCAGGC
TIMELESS	CCGCTATTTGAGGCATGAGG	GGCTGGTTGTGTCAAGTTCA
ASF1B	GATCCTAGACTCGGTGCTGG	TAGCCCACTCGGATGAACTC
HSPA5	AGGTAGAAAAGGCCAAACGG	ACTTTCTGGACGGGCTTCAT
IDH1	AGTGGCGGTTCTGTGGTAG	GCATCCTTGGTGACTTGGTC
APP	AACCAACCAGTGACCATCCA	CGCAAACATCCATCCTCTCC
IFIT1	CCTGGCTAAGCAAAACCCTG	CCAGCAGTGCAGAAAGTGAG

steine-Blocking Reagent for 10 min at room temperature (AB Sciex, Dublin, CA, USA) in dark. Then, the alkylated proteins were loaded into 10-KDa ultrafiltration tubes. After washing with 100 µl of tetraethyl-ammonium bromide (TEAB, 0.25 M), cells were collected by centrifugation at 12000 × g for 20 min. These procedures were replicated thrice. The proteins were dissolved with 50 µl of 0.5 M TEAB, and then subjected to hydrolysis with trypsin (Promega, Madison, WI, USA; dissolved in 50 mM acetic acid, trypsin: protein [w/w] =1:50) overnight at 37°C. The tryptic peptides were collected by centrifugation at 12,000 × g for 20 min, followed by freeze-drying in vacuum before processing with iTRAQ-8plex kit (AB Sciex, Dublin, CA, USA). 100 µg tryptic peptides were loaded with one unit of iTRAQ regent, followed by incubation for 2 h at room temperature. During iTRAQ tag process, the pH of solutions was assured to be 7.0-10.0. If the pH was less than 7.5, TEAB (1 M) was added to adjust the pH. Each sample was labeled with 2 tags (blank group: 113, 117; Iressa group: 114, 118; JDF12 group: 115, 119). All labeled peptides were pooled and freeze-dried in vacuum.

High pH reversed-phase fractionation

The pooled iTRAQ labeled peptides were dissolved with 150 µL of mobile phase A solution (20 mM $HCOONH_4$, pH 10), followed by centrifugation at 12,000 × g for 20 min. Then, the supernatant was loaded onto a column (Phenomenex columns; Gemini-NX 3u C18 110A; 150 × 2.00 mm, Torrance, CA, USA) and separated with a flow rate of 200 µL/min. The UV detection was done at wavelength of 214 nm/280 nm. The peptides were collected from a linear gradient formed with mobile phase A solution and mobile phase B solution (20 mM $HCOONH_4$, 80% CAN, pH 7.2). Collection was performed once every 1 min. According to the peak and time, 24 fractions of each sample were pooled and freeze-dried by vacuum centrifugation.

Reverse-phase LC-MS

Peptide sample was dissolved with a buffer (0.1% formic acid, 2% acetonitrile), and centrifuged at 12,000 × g for 20 min at 4°C. The supernatant was transferred to a chromatography column, and then eluted with a linear gradient of buffer A (0.1% formic acid) and buffer B (0.1% formic acid, 80% CAN) at a flow rate of 330 nL/min for a total of 60 min, and with an effective gradient (B phase from 4% to 50%) for 40 min. The separated peptides were directly transferred to a mass spectrometer (Thermo Scientific Q Exactive) for on-line detection. MS parameters: Resolution: 17,000; AGC target: $3e^6$, Maximum IT: 40 ms; Scan range: 350 to 1800 m/z; tandem MS parameters: Resolution: 17,500; AGC target: $1e^5$; Maximum IT: 60 ms; Top N: 20, NCE/stepped NCE: 30.

Protein identification and quantification

Protein identification and quantification were performed with ProteinPilot™ Software 5.0 (AB SCIEX) including Paragon™ Algorithm (5.0.0.0, 4767) using the Uniprot/Swiss-Prot databases. Some parameters for searching were as follows: Protein Detection Threshold [Unused ProtScore (Conf)]: > 0.05 (10.0%); Competitor Error Margin (ProtScore): 2.00; Revision Number: 4769; Annotations Retrieved from UniProt: No; Sample Type: iTRAQ 8 plex (Peptide Labeled); Cys. Alkylation: MMTS; Digestion: Trypsin; Instrument: Orbi MS (1-3 ppm), Orbi MS/MS; Special Factors: No; Species: No; ID Focus: Biological modifications; Database: TrSp_HUMAN.05.12.25.fasta; Search Effort: Thorough; FDR Analysis: Yes; User Modified Parameter Files: No. After searching, unused confidence score ≥ 1.3 and confidence level ≥ 95% were uses as qualification criteria of peptide. Proteins with at least three peptides and false discovery rate (FDR) < 1% were accepted. The proteins with poor repeatability (coefficient of variation [CV] > 0.5) or without quantitative information were removed. Base on the above available proteins, average fold change ≥ 1.5 was used as a threshold for up-regulation and average fold change ≤ 0.67 for down-regulation.

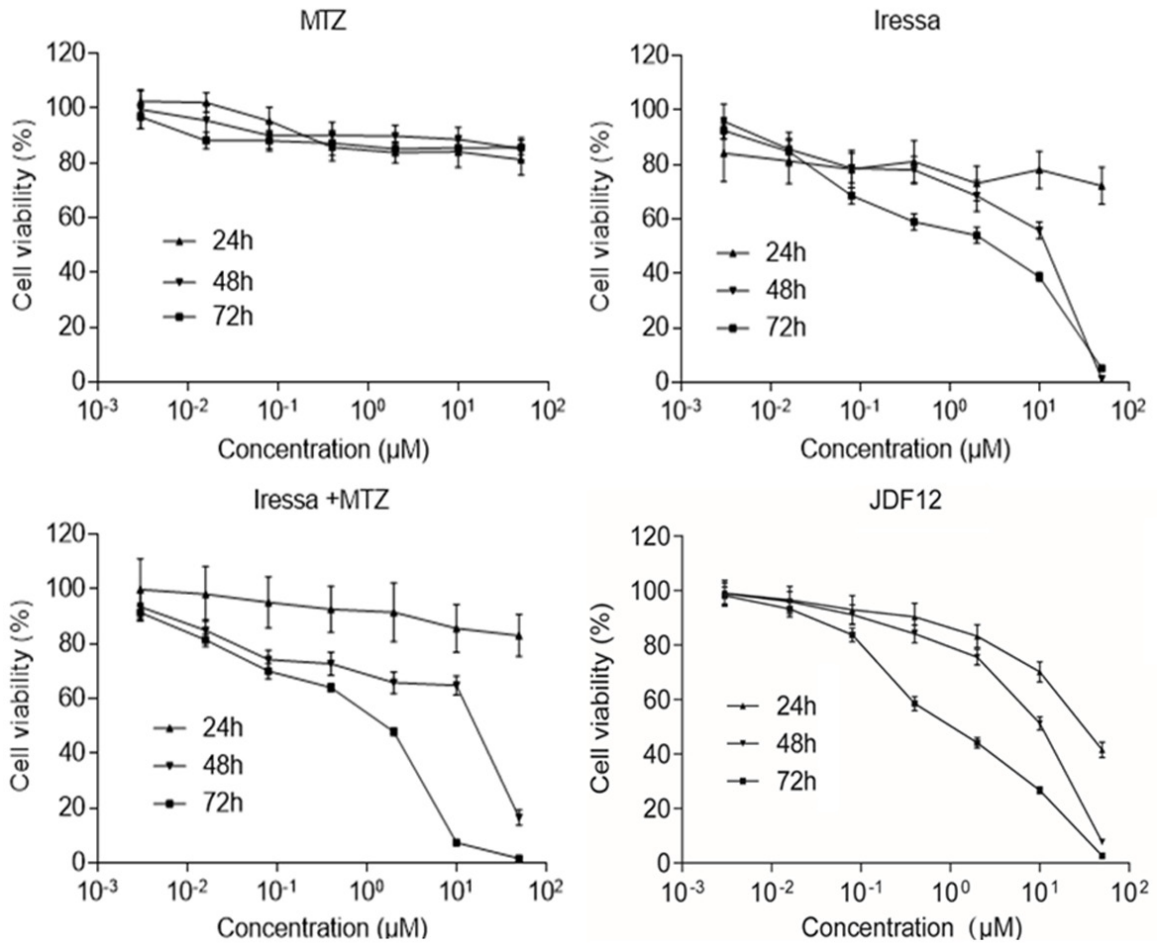

Figure 1. Cytotoxicity of MTZ, Iressa, Iressa plus MTZ and JDF12 on DU145 cells. Cells were exposed to MTZ, Iressa, Iressa plus MTZ and JDF12 for 24 h, 48 h, and 72 h. Growth inhibition was measured by MTT assay. Data are present as mean ± SD from 3 experiments.

Gene ontology and KEGG pathway enrichment analysis

The differentially expressed proteins were analyzed using web-based GO software (http://www.geneontology.org) for gene ontology (GO) annotation and enrichment analysis in order to better understand the biological functions of these proteins. Biological process, cellular component and molecular function are the main modules in the GO system. Pathway analysis was done using the web-based Kyoto Encyclopedia of Genes and Genomes (KEGG, http://www.kegg.jp). Hierarchical clustering was performed using Cluster 3.0, and the results were presented using java Tree view. Protein-protein interaction networks were built based on the publicly available program, and the Search Tool for the Retrieval of Interacting Genes/Proteins (STRING) database [8].

qPCR analysis

Total RNA was extracted from DU145 cells in different groups using the RNA extraction Kit (Takara) according to the manufacturer's instructions. Extracted RNA was reverse-transcribed with the Transcript or First Strand cDNA Synthesis Kit (Roche). The reaction was performed using Light Cycler 480 (Roche Diagnostics). β-actin was used as an internal reference. Primers used for qPCR were synthesized by Ruibotech (Beijing, China) and are list in **Table 1**. The relative RNA expression was calculated with $2^{-\Delta\Delta CT}$ method. The experiment was repeated three times.

Statistics

Data are presented as mean ± standard deviation (SD). All experiments were performed at

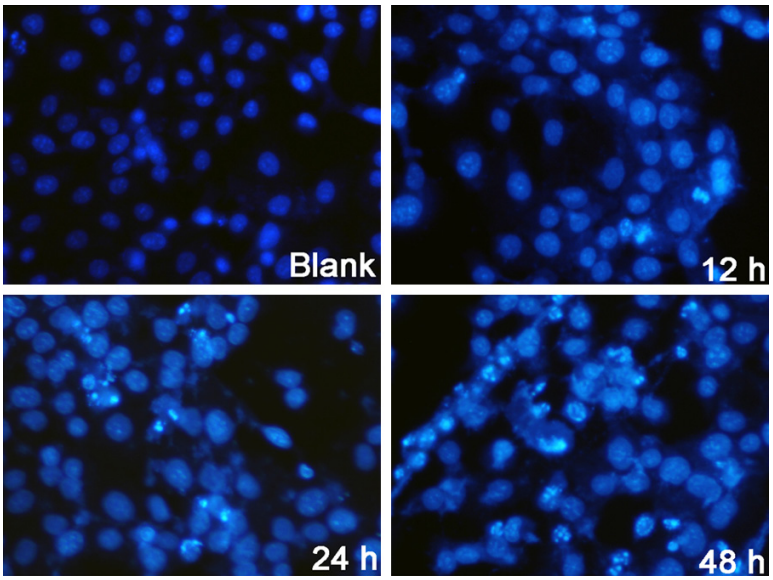

Figure 2. DAPI staining of apoptotic DU145 cells treated with IC_{50} JDF12 for 0 h, 12 h, 24 h, and 48 h. The apoptosis rate increased in a time-dependent manner.

least three times in triplicate. Statistical analysis was done with the GraphPad Prism v.5.01 software (GraphPad Prism software Inc., La Jolla, CA). Comparisons were done with student's t test. A value of $P < 0.05$ was considered statistically significant.

Results

JDF12 significantly inhibited the growth of DU145 cells

DU145 cells were treated with different concentrations of JDF12, Iressa, and MTZ for 24 to 72 h. MTT assay indicated a dose-related and time-related inhibition of DU145 cells proliferation (**Figure 1**). JDF12 cytotoxicity was more evident than MTZ, Iressa, and Iressa + MTZ group, the IC_{50} at 48 h was as follow: Iressa =12.79 ± 2.66 μM, Iressa + MTZ =10.80 ± 3.35 μM and JDF12 =7.31 ± 0.45 μM. IC_{50} of MTZ could not be measured in this study within 72 h, but was measured after treatment for more than 72 h in our previous studies [6, 7]. At the same time, most cells in JDF12 and Iressa groups became apoptotic when treatment was longer than 72 h. Taking these factors into consideration, IC_{50} at 48 h was used in this study.

JDF12 induced apoptosis of DU145 cells

To characterize JDF12-induced cell death, the nuclear chromatin condensation and fragmentation of DNA, a hallmark of apoptosis, was detected by DAPI staining. Compared with blank cells, cells exposed to IC_{50} JDF12 for 12 h, 24 h, and 48 h presented chromatin condensation and DNA fragmentation, indicating cell apoptosis (**Figure 2**). The apoptosis rate increased in a time-dependent manner.

Effect of JDF12 on DU145 cell cycle distribution

DU145 cells were exposed to IC_{50} JDF12 and cell cycle was detected by flow cytometry. As shown in **Figure 3**, the proportion of cells was 0%, 0.9%, 3.5%, and 22.1% in sub-G1 phase; 57.1%, 63.2%, 65.4%, and 57.6% in G1 phase; 26.6%, 28.8%, 21.8%, and 16.8% in S phase; 16.3%, 7.1%, 8.3%, and 4.5% in G2/M phase following exposure to IC_{50} JDF12 for 0 h, 12 h, 24 h, and 48 h, respectively. The proportion of cells in sub-G1 phase of JDF12 treated groups gradually increased as compared to blank group, suggesting that the genomic DNA fragmentation increased in a time-manner. Besides, the proportion of cells in G1 phase after JDF12 treatment was higher than that in blank group, and the proportion of cells in G2/M phase decreased gradually.

Protein identification and quantification

To understand the proteomic profiles between JDF12 and Iressa treated PCa cells, iTRAQ-based quantitative proteomic approach was employed. In total, 5071 proteins were identified, of which 42 proteins were identified as differentially expressed proteins between JDF12/Iressa (JDF12_vs_Iressa) and between JDF12/blank (JDF12_vs_blank), and included 21 up-regulated and 21 down-regulated proteins (Supplementary File 1).

GO annotation and KEGG analysis of differentially expressed proteins

To obtain a comprehensive view of the differentially expressed proteins, GO analysis was done using GO seq R package. The top 10 enriched GO terms within each major functional category

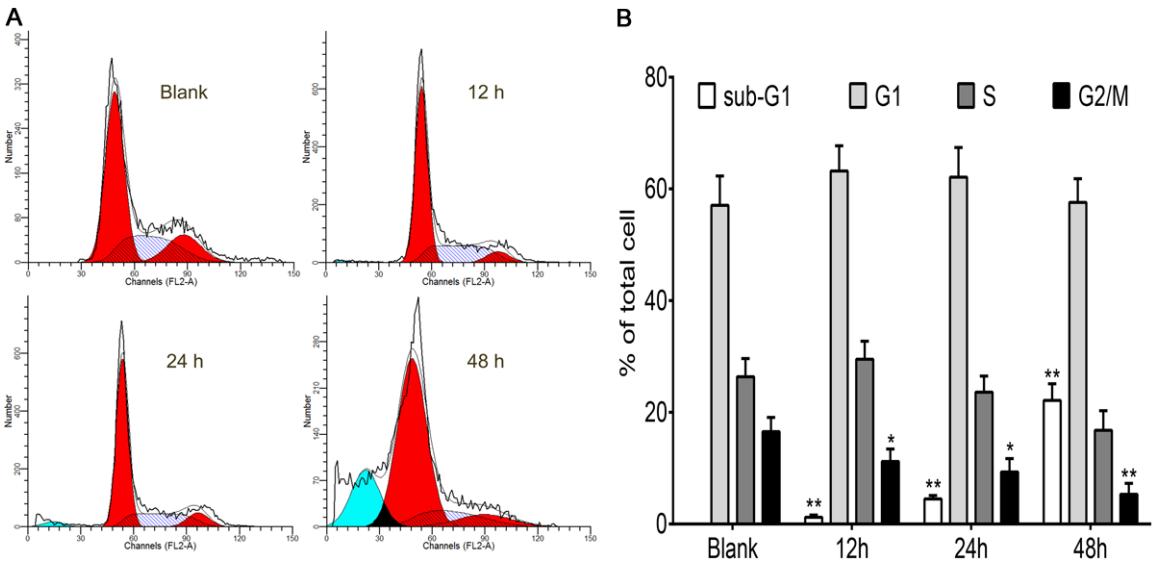

Figure 3. A: DU145 were treated with IC_{50} JDF12 for various period of times, then stained with PI and analyzed of the DNA content by flow cytometry. B: The proportion (± SD) of each cell phase was presented three independent experiments. Results showed that the genomic DNA fragmentation increased in a time-manner. One-way ANOVA analysis was used to compare between treatment groups. *P < 0.05, **P < 0.01.

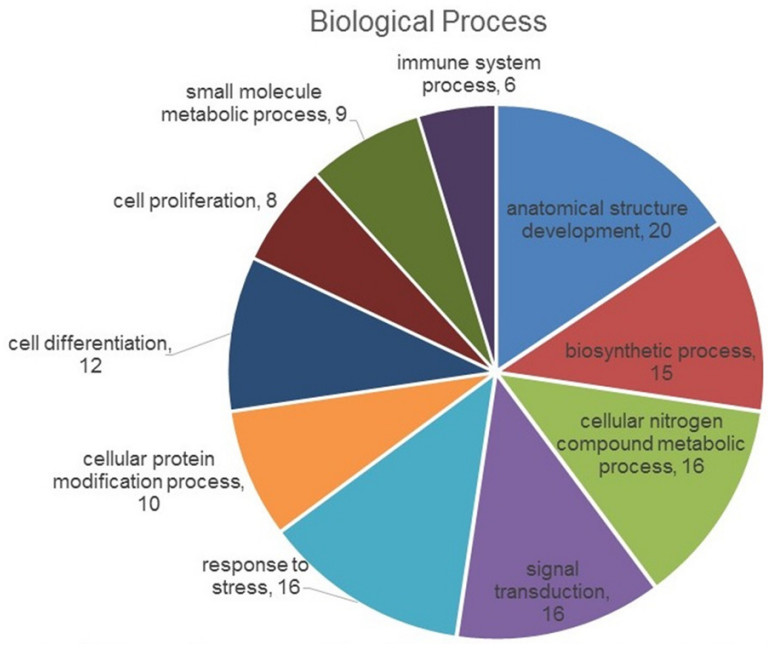

Figure 4. GO annotation analysis of the differentially expressed proteins. Top 10 enriched GO terms under "biological process". Part of the most enriched GO terms under "biological process" included "biosynthetic process", "cellular nitrogen compound metabolic process", "anatomical structure development", "cell cycle", etc.

are partly shown in **Figure 4**. Part of the most enriched GO terms under "biological process" included "biosynthetic process", "cellular nitrogen compound metabolic process", "anatomical structure development", "cell cycle", etc.

Differentially expressed proteins were also mapped to reference pathways in the KEGG database. Seventy-five proteins had a KEGG Orthology (KO) ID and were involved in 133 pathways in JDF12_vs_blank; while in JDF12_vs_Iressa, 92 differentially expressed proteins were found in 115 pathways (Supplementary Files 2 and 3).

The 42 proteins with differential expression both in JDF12_vs_Iressa and JDF12_vs_blank were classified into different groups: 1) DNA damage/repair (n=5); 2) apoptosis (n=7); 3) cell cycle-related (n=5); 4) energy metabolism (n=6); 5) calium homeostasis (n=1); 6) oxidative stress (n=4); 7) endoplasmic reticulum stress (n=2); 8) autophagy (n=1); 9) other proteins (e.g., nuclear regulating proteins and proteins of unknown function) (**Figure 5** and **Table 2**).

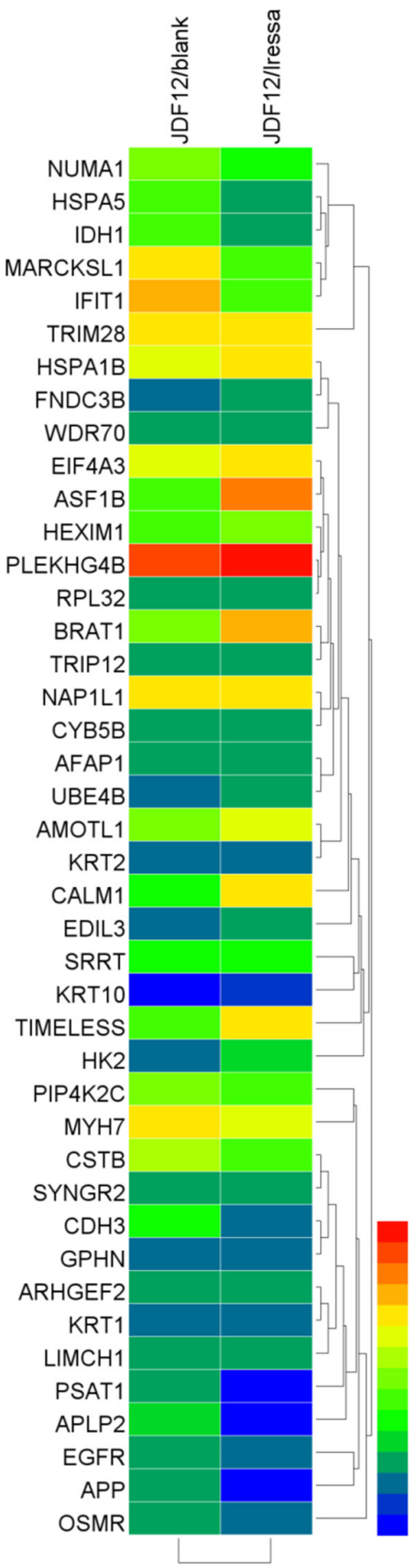

Figure 5. Heat map of proteins with significantly altered expression in JDF12/blank group and JDF12/Iressa group (Heatmap Illustrator). 42 proteins with differential expression both in JDF12_vs_Iressa and JDF12_vs_blank were classified into different groups.

Protein-protein interaction analysis of differentially expressed proteins

The protein-protein interaction (PPI) network analysis of the differentially expressed proteins was performed by using STRING 10. Results are shown in **Figure 6**. IFIT1, EGFR, HSPA5, IDH1, HK2, APP, and TIMELESS were proteins with higher connectivity in the network and play important roles in the regulation network (Supplementary File 4). Thus, they were selected for validation by qPCR.

Validation of differentially expressed proteins by qPCR

qPCR was employed to validate findings from iTRAQ findings. The mRNA expression of 7 proteins was detected, including HK2, TIMELESS, ASF1B, HSPA5, IDH1, APP, and IFIT1. The expression of TIMELESS, ASF1B, HSPA5, IDH1, and IFIT1 was up-regulated in JDF12 treated cells, and that of HK2 and APP was down-regulated in JDF12 treated cells, which were consistent with results from iTRAQ. However, the expression of HSPA5 and APP in Iressa group was opposite to that in iTRAQ (**Figure 7**).

Discussion

JDF12 may intervene with multiple signaling pathways, including those related to cell survival, apoptosis and DNA repair after injury, and then inhibits or delays the progression of PCa. Currently, DNA-alkylating agents are not the first- or second-line treatment in the guideline for the treatment of most cancers, and thus few studies focus on the mechanisms underlying the therapeutic effects of DNA-alkylating agents. Our study on JDF12 indicated that, with the assistance of EGFR-blocker, DNA-alkylating reagent showed a better performance in the treatment of PCa.

Both DNA-alkylating gents and EGFR-blockers are commonly used in the cancer therapy, while their limitations prevent them from further development. The limited clinical efficacy of anti-

Table 2. Differentially expressed proteins in JDF12/blank group and JDF12/Iressa group

Swiss Prot ID	Gene	Protein name	JDF12/blank Mean	JDF12/Iressa Mean	Biological Function
Q14980	NUMA1	Nuclear mitotic apparatus protein 1	1.73	1.58	Cell cycle
P11021	HSPA5	78 kDa glucose-regulated protein	1.67	0.51	Protein folding, endoplasmic reticulum stress, apoptotic process
Q13263	TRIM28	Transcription intermediary factor 1-beta	2.00	2.00	DNA repair
A0A0G2JIW1	HSPA1B	Heat shock 70 kDa protein 1B	1.97	2.12	Protein folding
P38919	EIF4A3	Eukaryotic initiation factor 4A-III	1.91	2.21	RNA processing, regulation of translation
O75874	IDH1	Isocitrate dehydrogenase [NADP] cytoplasmic	1.62	0.63	Tricarboxylic acid cycle, oxidative stress
Q9BXP5	SRRT	Serrate RNA effector molecule homolog	1.52	1.53	Transcription, gene silencing by RNA
H0YIV4	NAP1L1	Nucleosome assembly protein 1-like 1	2.17	2.99	Nucleosome assembly
P62158	CALM1	Calmodulin	1.55	2.05	Glycogen catabolic process, calcium ion, homeostasis
Q8TBX8	PIP4K2C	Phosphatidylinositol 5-phosphate 4-kinase type-2 gamma	1.70	1.64	Autophagy, phosphatidylinositol, metabolic process
Q6PJG6	BRAT1	BRCA1-associated ATM activator 1	1.79	3.84	Glucose metabolic process, apoptotic process, DNA damage repair
P49006	MARCKSL1	MARCKS-related protein	2.02	1.60	Protein phosphorylation, regulation of proliferation
Q9UNS1	TIMELESS	Protein timeless homolog	1.58	2.51	DNA replication, cell cycle, DNA repair
Q9NVP2	ASF1B	Histone chaperone ASF1B	1.63	4.08	Nucleosome assembly, transcription, chromatin, modificatin
O94992	HEXIM1	Protein HEXIM1	1.65	1.75	Transcription, p53 signal transduction
P04080	CSTB	Cystatin-B	1.83	1.65	Proteolysis
P22223	CDH3	Cadherin-3	1.54	0.46	Response to stress, cell adhesion, signal transduction
P09914	IFIT1	Interferon-induced protein with tetratricopeptide repeats 1	3.46	1.66	Immune response
P12883	MYH7	Myosin-7	2.11	1.94	Muscle contraction, ATP metabolic process
Q8IY63	AMOTL1	Angiomotin-like protein 1	1.71	1.94	Signal transduction
Q96HN1	PLEKHG4B	PLEKHG4B protein	10.23	21.56	Unknown
Q92974	ARHGEF2	Rho guanine nucleotide exchange factor 2	0.65	0.62	Cell cycle, cell proliferation, apoptotic process, GTPase activity
P00533	EGFR	Epidermal growth factor receptor	0.56	0.49	EGFR signaling pathway, oxidative stress, cell proliferation, cell migration, cell cycle, apoptotic process, DNA repair
Q9UPQ0	LIMCH1	LIM and calponin homology domains-containing protein 1	0.61	0.55	Actomyosin structure organization
Q9Y617	PSAT1	Phosphoserine aminotransferase	0.60	0.26	Amino biosynthetic process
F5H039	GPHN	Gephyrin	0.48	0.40	Biosynthetic process
Q14669	TRIP12	E3 ubiquitin-protein ligase TRIP12	0.51	0.56	Double-strand break repair, protein ubiquitination
P13645	KRT10	Keratin, type I cytoskeletal 10	0.27	0.30	Keratinocyte differentiation
P04264	KRT1	Keratin, type II cytoskeletal 1	0.45	0.42	Oxidative stress, complement activation, angiogenesis
P35908	KRT2	Keratin, type II cytoskeletal 2 epidermal	0.45	0.47	Keratinization
Q9NW82	WDR70	WD repeat-containing protein 70	0.56	0.59	Biosynthetic process
P05067	APP	Amyloid beta A4 protein	0.50	0.27	Translation, endocytosis, apoptotic process, oxidative stress, immune response, cell cycle, gluconeogenesis
P52789	HK2	Hexokinase-2	0.44	0.66	Glycolytic process, apoptotic processing
Q8N556	AFAP1	Actin filament-associated protein 1	0.56	0.63	Cytoskeleton organization, signal transduction
O95155	UBE4B	Ubiquitin conjugation factor E4 B	0.38	0.54	Protein polyubiquitination, apoptotic process, endoplasmic reticulum stress
Q06481	APLP2	Amyloid-like protein 2	0.66	0.24	Peptidase activity, G-protein coupled receptor signaling pathway

Q99650	OSMR	Oncostatin-M-specific receptor subunit beta	0.58	0.49	Cell proliferation, inflammatory response
J3KNF8	CYB5B	Cytochrome b5 type B	0.56	0.64	Catalytic activity
043760	SYNGR2	Synaptogyrin-2	0.50	0.50	Regulate membrane traffic in non-neuronal cells
F8W727	RPL32	60S ribosomal protein L32	0.50	0.60	Translation
043854	EDIL3	EGF-like repeat and discoidin I-like domain-containing protein 3	0.46	0.52	Cell adhesion
Q53EP0	FNDC3B	Fibronectin type III domain-containing protein 3B	0.44	0.54	Regulator of adipogenesis

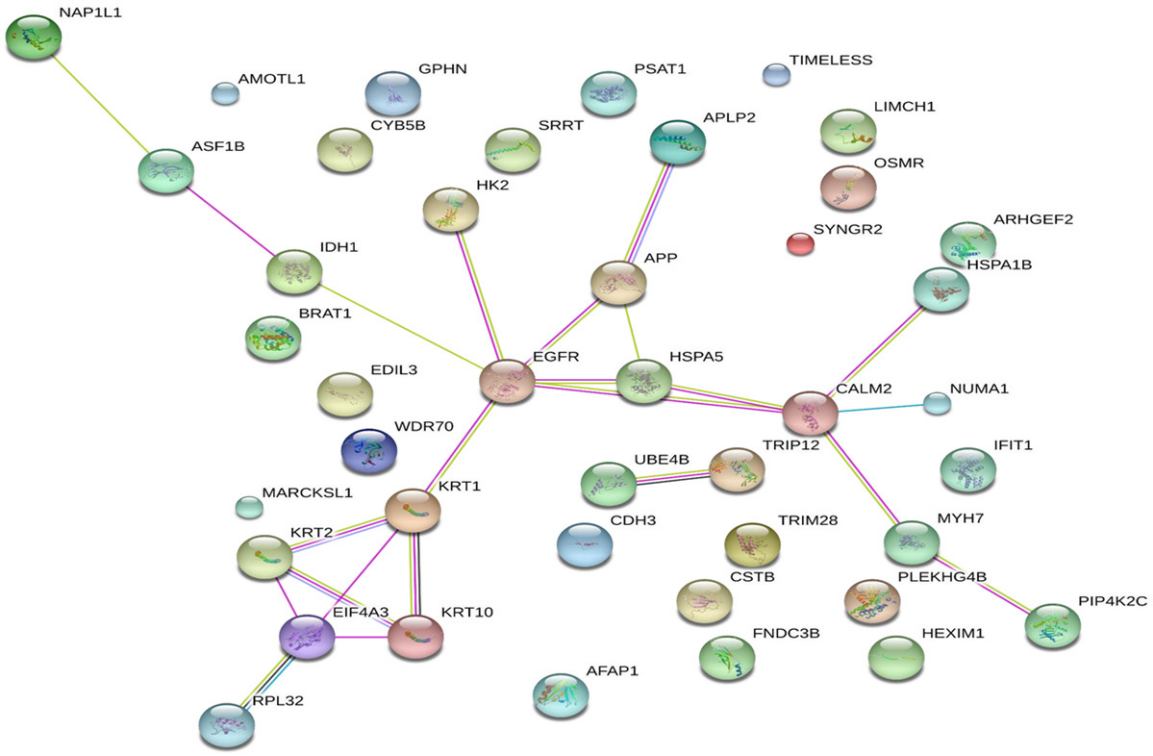

Figure 6. The protein-protein interaction (PPI) network of differentially expressed proteins identified in DU145 cells (STRING 10). IFIT1, EGFR, HSPA5, IDH1, HK2, APP, and TIMELESS are proteins with higher connectivity in the network.

cancer drugs can be attributed, at least in part, to their inability to kill a sufficient number of cancer cells without causing toxicity. A combi-targeting molecule combines the advantages of single molecule, and at the same time, lessens the disadvantages of single molecule [6]. However, it is a long way to clarify the specific mechanisms of therapeutic effects of a combi-targeting molecule. In our previous study, better anti-tumor effects were achieved after treatment with JDF12, a combi-targeting molecule [6, 7], which was further confirmed in this study. However, the exact mechanisms of its anti-tumor effect are still poorly understood.

Cytotoxic drugs that target DNA are widely used in cancer therapy by affecting the DNA damage/repair [9]. Protein TIMELESS homolog is one of the proteins with close relationship with DNA repair/damage [10]. Previous studies have shown that TIMELESS can form a physical and functional interaction with DDX11 and act in concert to preserve the replication fork progression in perturbed conditions [10]. It has also been shown that to maintain chromosome integrity is very important during and after replication, with roles in the coordination of leading and lagging-strand polymerases, the establishment of sister chromatid cohesion, the

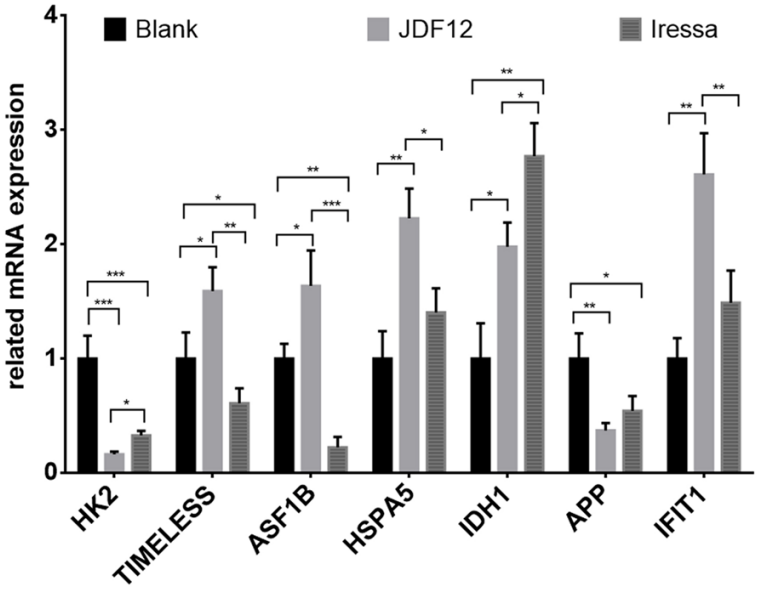

Figure 7. Validation of mRNA expressions of HK2, TIMELESS, ASF1B, HSPA5, IDH1, APP, and IFIT1 by qPCR. Expressions of these proteins except HSPA5 and APP were consistent with results from iTRAQ. *P < 0.05, **P < 0.01, ***P < 0.001.

preservation of fork integrity at replication barriers, and prevention of genome rearrangement [11]. TIMELESS expression was up-regulated in JDF12 group, while down-regulated in Iressa group when compared with blank group (**Figure 5** and **Table 2**). The effects of JDF12 on cell cycle and cell growth may be responsible for this phenomenon. The proportion of cells in G1 phase increased markedly, and the growth of most cells was significantly inhibited by JDF12. The expression of TIMELESS would be higher than in blank group and Iressa group, However, the exact role of TIMELESS in PCa is still unclear.

Histone chaperone ASF1B is another important protein involved in DNA damage/repair and also associated with DNA replication, cell cycle and DNA binding [12, 13]. The over-expression of ASF1B has been found in some cancers, including breast cancer and multiple myeloma [12, 14]. In addition, the expression of ASF1B is also related to miR-214 and P53 mRNA, which may influence DNA repair/damage [12]. The expression of ASF1B was similar to that of TIMELESS (**Figure 5** and **Table 2**), and its effects might be also similar to that of TIMELESS.

Among most cancer studies [7, 12, 14], the expression of proteins related to DNA damage/repair is down-regulated. However, in our study, all proteins except for EGFR, a protein linked to DNA damage/repair, displayed up-regulated expression. DNA-alkylating agents act on DNA damage and repair. When EGFR-blocker was used alone, the expression of DNA damage/repair related proteins was down-regulated; when DNA-alkylation agent combined with EGFR blocker was used, the cancer cells suffered from serious DNA damage, and produced more proteins to repair DNA, leading to the elevated expression of proteins associated with DNA damage/repair. EGFR is a protein involved in DNA repair. If only DNA repair signaling pathway is considered, EGFR protein expression should be up-regulated. However, JDF12 is also a potent blocker of EGFR, which is more potent than its induced DNA repair, and thus the expression of EGFR was down-regulated.

Resistance to apoptosis is one of the most important mechanism of cancer cells escaping from non-immune surveillance of the host [15]. Apoptosis is the end-point of multiple pathways that lead to enzymatic breakdown of cellular DNA. In the present study, 7 proteins related to cell apoptosis were identified, including UBE4B, EGFR, HSPA5, APP, HK2, BRAT1, and ARHGEF2, after JDF12 treatment.

The expression of HSPA5, APP, and HK2 was further confirmed by qPCR. Lower expression of HSPA5 is associated with increased response to unfolded proteins, and may induce the autophagy and apoptosis of cancer cells [16]. Although the expression of HSPA5 in JDF12 group was higher when compared with blank group, it was lower than that in Iressa group. With the assistance of EGFR-blocker, DNA-alkylating reagent had better performance in inducing apoptosis. The decreased HSPA5 expression may induce the autophagy and apoptosis of cancer cells.

A study on HK2 conditional knockout mice showed that HK2 was required for tumor initiation and maintenance in mouse models of Kras-driven lung cancer and ErbB2-driven breast cancer [17]. In another study focusing on castration-resistant PCa, HK2 was also over-expressed in castration-resistant PCa, which was related to Pten/p53 deficiency [18, 19]. The down-regulated HK2 expression as well as inhibited cells growth in the present study mean JDF12 may inhibit the growth of CRPC cells and delay the progression of PCa via a Pten/P53 dependent manner, but the specific mechanisms underlying the effects of JDF12 on this pathway should be further explored.

The expression of UBE4B, EGFR, APP, BRAT1, and ARHGEF2 that associated with apoptosis was also detected in this study. All proteins except BRCA1-associated ATM activator 1 showed down-regulated expression as HSPA5, which increased the apoptosis of cancer cells. BRAT1 is not only associated with apoptosis, but also with DNA damage/repair, and energy metabolism [20, 21]. There is a network in the interaction among proteins, and we can not consider a single pathway involved in the effects of JDF12.

The regulation of cell cycle is closely related to cell survival and determines the cell fate [22]. In our study, JDF12 was found to increase the proportion of cells in G1 phase as compared to blank group, and the proportion of cells in mitosis (G2/M) phase was decreased gradually. 5 proteins related to cell cycle, including EGFR, APP, NUMA1, ARHGEF2, and TIMELESS, were identified as differentially expressed proteins. Only TIMELESS and NUMA1 showed up-regulated expression in JDF12 group, and the expression of remaining 3 proteins was down-regulated in Iressa group, and greater decrease was noted in JDF12 group. NUMA1 is a protein known to be crucial for the proper positioning of the mitotic spindle in polarized cells and may affect the cell cycle transition [23]. A study indicates that the cell cycle can control DNA repair [24]. The correct duplication and transmission of genetic material to daughter cells are the primary objectives of the cell division.

Energy metabolism also plays an important role in the progression of cancers. Cell can not live without energy metabolism. In our study, 6 differentially expressed proteins were identified to be related to energy metabolism, and most of them also took part in other pathways, including IDH1, APP, HK2, BRAT1, and CALM1. For example, IDH1 may cause DNA aberrance and histone methylation and is closely related to hematological and neural malignancies [25]. In Frank's studies [26], IDH1 was also found to be associated with cellular energy metabolism and could promote anabolic metabolism and angiogenesis. Although the expression of IDH1 was up-regulated in JDF12 group when compared with blank group, it was down-regulated when compared with Iressa group, which means DNA-alkylating agent may decrease the expression of IDH1.

Some proteins that associated with autophagy, endoplasmic reticulum stress, oxidative stress, and calcium homeostasis were also identified in this study. These proteins may also influence the development of cancer cells, and some of them have other functions.

This study tried to clarify the mechanism underlying the anti-tumor effect of JDF12, a combi-target molecule of DNA-alkylating agent and EGFR-blocker, by iTRAQ and qPCR. However, the molecular mechanisms underlying the pathogenesis of cancer are too complex to understand. The mechanisms mentioned above were only a small part in the pathogenesis of cancers, and it will cost a long time to explore the unknown area. None of the pathways above can explain the whole pathogenesis of PCa without the assistant of other pathways because they form a network to influence the growth of cancer cells.

Conclusion

This study for the first time investigated the anti-tumor effects of combi-target molecule JDF12 and DNA-alkylating agent by protemics profiling, which brings light to the use of DNA-alkylating agents in the therapy of cancers. Proteins that are influenced by DNA-alkylating reagent and EGFR-blocker are also identified, which may help to clarify the mechanisms and provide new targets for cancer therapy. However, further studies are required to explore the exact mechanism underlying the effects of JDF12 at miRNA and gene levels.

Acknowledgements

This work was supported by the Science and Technology Planning Project of Guangzhou

(Grant No. 201704020052 to You-Qiang Fang), the Science and Technology Project of Guangdong (Grant No. 2013B021800084, to You-Qiang Fang), and the Fundamental Research Funds for the Central Universities (Grant No. 14YKPY25, to You-Qiang Fang).

Disclosure of conflict of interest

None.

Address correspondence to: You-Qiang Fang, Department of Urology, The Third Affiliated Hospital of Sun Yat-sen University, Guangzhou 510630, China. E-mail: Fang_1573@126.com

References

[1] Attard G, Parker C, Eeles RA, Schroder F, Tomlins SA, Tannock I, Drake CG and de Bono JS. Prostate cancer. Lancet 2016; 387: 70-82.

[2] Siegel RL, Miller KD and Jemal A. Cancer statistics, 2016. CA Cancer J Clin 2016; 66: 7-30.

[3] Lowrance WT, Roth BJ, Kirkby E, Murad MH and Cookson MS. Castration-resistant prostate cancer: AUA guideline amendment 2015. J Urol 2016; 195: 1444-1452.

[4] Maroto P, Solsona E, Gallardo E, Mellado B, Morote J, Arranz JA, Gomez-Veiga F, Unda M, Climent MA and Alcaraz A. Expert opinion on first-line therapy in the treatment of castration-resistant prostate cancer. Crit Rev Oncol Hematol 2016; 100: 127-136.

[5] Buchanan MK, Needham CN, Neill NE, White MC, Kelly CB, Mastro-Kishton K, Chauvigne-Hines LM, Goodwin TJ, McIver AL, Bartolotti LJ, Frampton AR, Bourdelais AJ and Varadarajan S. Glycoconjugated site-selective DNA-methylating agent targeting glucose transporters on glioma cells. Biochemistry 2017; 56: 421-440.

[6] Fang Y, Qiu Q, Domarkas J, Larroque-Lombard AL, Rao S, Rachid Z, Gibbs BF, Gao X and Jean-Claude BJ. "Combi-targeting" mitozolomide: conferring novel signaling inhibitory properties to an abandoned DNA alkylating agent in the treatment of advanced prostate cancer. Prostate 2012; 72: 1273-1285.

[7] Fang Y, Wu J, Li T, Luo Y, Qiu Q, Quan X, Gao L and Liu W. Biological effects of novel "combi-targeting" molecule and its effect on DNA repair pathway in hormone-refractory prostate cancer. Am J Cancer Res 2015; 5: 2387-2395.

[8] Zhou CX, Zhu XQ, Elsheikha HM, He S, Li Q, Zhou DH and Suo X. Global iTRAQ-based proteomic profiling of toxoplasma gondii oocysts during sporulation. J Proteomics 2016; 148: 12-19.

[9] Valdez BC, Nieto Y, Murray D, Li Y, Wang G, Champlin RE and Andersson BS. Epigenetic modifiers enhance the synergistic cytotoxicity of combined nucleoside analog-DNA alkylating agents in lymphoma cell lines. Exp Hematol 2012; 40: 800-810.

[10] Cali F, Bharti SK, Di Perna R, Brosh RM Jr and Pisani FM. Tim/Timeless, a member of the replication fork protection complex, operates with the Warsaw breakage syndrome DNA helicase DDX11 in the same fork recovery pathway. Nucleic Acids Res 2016; 44: 705-717.

[11] Borde V and Lichten M. A timeless but timely connection between replication and recombination. Cell 2014; 158: 697-698.

[12] Misiewicz-Krzeminska I, Sarasquete ME, Quwaider D, Krzeminski P, Ticona FV, Paino T, Delgado M, Aires A, Ocio EM, Garcia-Sanz R, San Miguel JF and Gutierrez NC. Restoration of microRNA-214 expression reduces growth of myeloma cells through positive regulation of P53 and inhibition of DNA replication. Haematologica 2013; 98: 640-648.

[13] Paul PK, Rabaglia ME, Wang CY, Stapleton DS, Leng N, Kendziorski C, Lewis PW, Keller MP and Attie AD. Histone chaperone ASF1B promotes human beta-cell proliferation via recruitment of histone H3.3. Cell Cycle 2016; 15: 3191-3202.

[14] Corpet A, De Koning L, Toedling J, Savignoni A, Berger F, Lemaitre C, O'Sullivan RJ, Karlseder J, Barillot E, Asselain B, Sastre-Garau X and Almouzni G. Asf1b, the necessary Asf1 isoform for proliferation, is predictive of outcome in breast cancer. Embo J 2011; 30: 480-493.

[15] Bhutia SK, Mallick SK and Maiti TK. Tumour escape mechanisms and their therapeutic implications in combination tumour therapy. Cell Biol Int 2010; 34: 553-563.

[16] Cerezo M and Rocchi S. New anti-cancer molecules targeting HSPA5/BIP to induce endoplasmic reticulum stress, autophagy and apoptosis. Autophagy 2017; 13: 216-217.

[17] Patra KC, Wang Q, Bhaskar PT, Miller L, Wang Z, Wheaton W, Chandel N, Laakso M, Muller WJ, Allen EL, Jha AK, Smolen GA, Clasquin MF, Robey RB and Hay N. Hexokinase 2 is required for tumor initiation and maintenance and its systemic deletion is therapeutic in mouse models of cancer. Cancer Cell 2013; 24: 213-228.

[18] Deng Y and Lu J. Targeting hexokinase 2 in castration-resistant prostate cancer. Mol Cell Oncol 2015; 2: e974465.

[19] Wang L, Wang J, Xiong H, Wu F, Lan T, Zhang Y, Guo X, Wang H, Saleem M, Jiang C, Lu J and Deng Y. Co-targeting hexokinase 2-mediated Warburg effect and ULK1-dependent autophagy suppresses tumor growth of PTEN- and TP53-deficiency-driven castration-resis-

tant prostate cancer. EBioMedicine 2016; 7: 50-61.
[20] Low LH, Chow YL, Li Y, Goh CP, Putz U, Silke J, Ouchi T, Howitt J and Tan SS. Nedd4 family interacting protein 1 (Ndfip1) is required for ubiquitination and nuclear trafficking of BRCA1-associated ATM activator 1 (BRAT1) during the DNA damage response. J Biol Chem 2015; 290: 7141-7150.
[21] So EY and Ouchi T. BRAT1 deficiency causes increased glucose metabolism and mitochondrial malfunction. BMC Cancer 2014; 14: 548.
[22] Soufi A and Dalton S. Cycling through developmental decisions: how cell cycle dynamics control pluripotency, differentiation and reprogramming. Development 2016; 143: 4301-4311.
[23] Metodieva G, Adoki S, Lausen B and Metodiev MV. Decreased usage of specific scrib exons defines a more malignant phenotype of breast cancer with worsened survival. EBioMedicine 2016; 8: 150-158.
[24] Hustedt N and Durocher D. The control of DNA repair by the cell cycle. Nat Cell Biol 2016; 19: 1-9.
[25] Yao L, Barontini M, Niederle B, Jech M, Pfragner R and Dahia PL. Mutations of the metabolic genes IDH1, IDH2, and SDHAF2 are not major determinants of the pseudohypoxic phenotype of sporadic pheochromocytomas and paragangliomas. J Clin Endocrinol Metab 2010; 95: 1469-1472.
[26] Schaap FG, French PJ and Bovee JV. Mutations in the isocitrate dehydrogenase genes IDH1 and IDH2 in tumors. Adv Anat Pathol 2013; 20: 32-38.